Further Results on the Accessibility of a Satellite with Two Reaction Wheels

Frédéric Boyer and Mazen Alamir

Abstract- **This article deals with the attitude open loop control of a satellite actuated by two reaction wheels and contributes to answer to the question of [1]: "what is the most one can expect in such a case?" As a matter of fact, the satellite with two reaction wheels is not controllable on the whole state space of the spacecraft attitudes. Nevertheless, a five dimensional sub-manifold is susceptible to be accessible from any state. In this article, this sub-manifold will be exhibited and two control objectives related to it, will be studied. The first one corresponds to steer the satellite from any attitude state to any state at rest. The second one corresponds to steer the spacecraft from any state to a given configuration with a constant spin about the unactuated spacecraft axis. More than giving qualitative answers, the article gives constructive demonstrations of accessibility since it exhibits explicit open loop control laws based on a path planning compatible with these two objectives. Finally, some simulation results illustrate the feasibility of the approach.**

I. INTRODUCTION

Technologically, the actuators used for attitude satellite control, are the most of the time realized by momentum exchange devices or gas jet propellers. In despite of their apparent resemblance, the problem of control raised by these two types of technology are drastically different. As a matter of fact, in the first case, the satellite changes its attitude by inertial transfers via a momentum conservation law as in the case of a "falling cat" [2], while in the second, it moves thanks to reaction forces generating actual external torques. What ever be the type of actuators, the first works about attitude control in the case of actuator failures dealt with some questions of controllability and were probably due to Bonnard [3] and Crouch [4]. In particular, the second author showed that in the case of a satellite actuated with momentum wheels, controllability fails in the case of fewer than three actuators. This is probably why the control community primarily investigated the case of spacecraft under-actuated with gas jets [1,5-7].

In this paper, we focus our attention on the attitude open loop control of a satellite actuated with two inertia wheels. In this case, if the satellite is in general not controllable, any attitude remains accessible at rest when the satellite total momentum is zero. Thus, the most of the solutions today proposed for controlling the satellite with two rotors deal with the stabilization in this restricted case. Moreover, because dynamics does not respect the Brockett's condition, they are time varying feedback or non-smooth ones [8,9]. Contrarily to these results we here consider the general case where the satellite has not forcedly a

zero total angular momentum. In these conditions, we shall prove that the failure of a rotor imposes a non-holonomic constraint forcing the admissible spacecraft state space to be a five dimensional sub-manifold of $TSO(3)$. This constraint will be used to define two types of objectives compatible with it, while being relevant with practical applications. In the first one, the final velocity is imposed to be zero, while in the second, this is the final attitude that is arbitrary fixed. Moreover, we shall prove that these two objectives are accessible from any states of the admissible state space.

More than giving qualitative results to the accessibility problem, the article proposes an explicit constructive procedure for deriving open loop steering laws. This procedure is based on the definition of two variables whose time evolution allows reconstructing all the state variables and finally the control torques. Note here that in despite of their similarities, these variables are not some "flat outputs" [10] since the reconstruction process is not only based on algebraic relations but also on differential ones. Moreover, the proposed solution is intimately funded on a geometrical insight of the problem, revealing the role of the curvature of the unit sphere in the control and exhibiting some "geometric phases" and "dynamic ones", as in the "falling cat problem".

The paper is structured as follows. First, the spacecraft attitude space $SO(3)$ will be replaced (section II) by the principal bundle $S^2 \times SO(2)$. The open loop control strategy will be presented in section III. In section IV, this control law is coupled to a path planning derived from a stereo-graphic chart of S^2 [11,12] and first restricted to one of its open sub-set. Finally, the section V deals with the singularities and extends the accessibility to the whole admissible space. Before concluding (VII) some simulation results are given in section VI.

II. MODELLING

II.1 Definitions and notations

We consider a satellite with two-inertia wheels (rotors) as displayed figure 1. Applying the standard parameterization of the rigid body to the rigid spacecraft, we define three frames. The first two are spatial ones, i.e., a fixed and a mobile one respectively denoted $(O,\boldsymbol{e}_1,\boldsymbol{e}_2,\boldsymbol{e}_3)$ and $(O,\boldsymbol{t}_1,\boldsymbol{t}_2,\boldsymbol{t}_3)$. The third ("material"): $(O_o,\boldsymbol{E}_1,\boldsymbol{E}_2,\boldsymbol{E}_3)$, is attached to the mater. It is related to the fixed spatial one through the choice of a reference configuration, here s.t.: $(O,\boldsymbol{e}_1,\boldsymbol{e}_2,\boldsymbol{e}_3)=(O_o,\boldsymbol{E}_1,\boldsymbol{E}_2,\boldsymbol{E}_3)$. The two spaces (material and spatial) are linked through the relation:

$$\boldsymbol{t}_i = \boldsymbol{R}.\boldsymbol{E}_i \ , \ i=1,2,3 \tag{1}$$

Where $\boldsymbol{R}=\boldsymbol{t}_i \otimes \boldsymbol{E}_i \in SO(3)$ is a rotation two-point tensor ("$\otimes$" denotes the usual tensor product). The vector of angles $q=(q_1,q_2)^T \in \mathbb{R}^2$, will parameterize the rotor dynamics. All over the article $\langle\ ,\ \rangle$ denotes the inner product on $\mathbb{R}^3$, and a

point marks the contracted product of any two tensors (as in (1)). Finally, $\hat{\boldsymbol{V}}$ is the skew-symmetric tensor paired to any $\boldsymbol{V} \in \mathbb{R}^3$, while $(\hat{\boldsymbol{V}})^{\vee} = \boldsymbol{V}$.

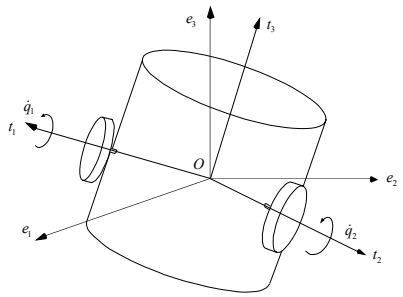

Figure 1: Satellite with two rotors

II.2 Geometric modeling

Because one of the three mobile axes (here $\boldsymbol{t}_3$) is distinguished (by its non actuated character), the isotropy of $SO(3)$ is lost and it is relevant to replace $SO(3)$ by its fibration (said of Stieffel [13]): $SO(3) = (SO(3)/SO(2)) \times SO(2)$. Moreover, the homogeneous space $SO(3)/SO(2)$ is isomorphic to S^2. Hence, $SO(3)$ is replaced by the principal fiber bundle $S^2 \times SO2$, with S^2 the base manifold, and $SO(2)$ the fiber. With such a choice, the spacecraft attitude splits into that[1] of $\boldsymbol{t}_3$ on S^2, plus the rotation about $\boldsymbol{t}_3$ parameterized by a single angle λ. Therefore, any $\boldsymbol{R}$ of (1) can be written:

$$\boldsymbol{R}(\boldsymbol{t}_3, \lambda) = \exp(\lambda \hat{\boldsymbol{t}}_3).\boldsymbol{\Lambda}_{\boldsymbol{E}_3}(\boldsymbol{t}_3) \tag{2}$$

Where $\boldsymbol{\Lambda}_{\boldsymbol{E}_3}$ is a diffeomorphism from an open set $\mathcal{U} \subset S^2$ to an open set $\mathcal{V} \subset SO(3)$. It represents any rotation parameterized by $\boldsymbol{t}_3$ s.t. $\boldsymbol{\Lambda}_{\boldsymbol{E}_3}(\boldsymbol{t}_3).\boldsymbol{E}_3 = \boldsymbol{t}_3$. Let us note first that there exist an infinity of maps $\boldsymbol{\Lambda}_{\boldsymbol{E}_3}(.)$, each one fixing a unique $\lambda(\boldsymbol{R})$. Furthermore, $\boldsymbol{\Lambda}_{\boldsymbol{E}_3}$ fixes an ortho-normed mobile frame [14]: $\boldsymbol{F}_{\boldsymbol{\Lambda}_{\boldsymbol{E}_3}} : \boldsymbol{t}_3 \mapsto (\tilde{\boldsymbol{X}}_\alpha)_{\alpha=1,2}$ on $T\mathcal{U} \subset TS^2$, defined by induction of the field: $\boldsymbol{X}_\alpha(\boldsymbol{t}_3) = \boldsymbol{\Lambda}_{\boldsymbol{E}_3}(\boldsymbol{t}_3).\boldsymbol{E}_\alpha$ of $\mathbb{R}^3$ into $T\mathcal{U}$. Therefore, every $\boldsymbol{\Lambda}_{\boldsymbol{E}_3}$, is distinguished by its $\boldsymbol{F}_{\boldsymbol{\Lambda}_{\boldsymbol{E}_3}}$. Hence, in order to explicit (2), we first define a chart on S^2, so fixing $\mathcal{U}$, and second: a mobile frame on $\mathcal{U}$. In the following, we shall use a spherical chart for tensor calculus purposes. In this case, parameterizing $\boldsymbol{t}_3$ as:

$$\boldsymbol{t}_3 = \sin\varphi \sin\psi\ \boldsymbol{e}_1 - \cos\varphi \sin\psi\ \boldsymbol{e}_2 + \cos\psi\ \boldsymbol{e}_3 \tag{3}$$

fixes $\boldsymbol{e}_3 \in S^2$ (respect., $-\boldsymbol{e}_3$) as the north pole (respect., south) of the chart $(\mathcal{U}, \varphi, \psi)$, with $\mathcal{U} = S^2 - \{\pm \boldsymbol{e}_3\}$. Moreover, fixing $\boldsymbol{\Lambda}_{\boldsymbol{E}_3}$ by:

$$\boldsymbol{\Lambda}_{\boldsymbol{E}_3}(\boldsymbol{t}_3) = \exp(\psi(\cos\varphi\ \boldsymbol{e}_1 + \sin\varphi\ \boldsymbol{e}_2)^{\wedge}).\exp(\varphi \hat{\boldsymbol{E}}_3) \tag{4}$$

[1] In the following our notations do not distinguish a point of S^2 from the unit vector of $\mathbb{R}^3$, associated to it.

fixes on: $\mathcal{V} := SO(3) - \mathcal{U}_{\pm}$, with: $\mathcal{U}_{\pm} := \{\boldsymbol{R}_{\pm} \in SO(3) / \ \boldsymbol{R}_{\pm} = \boldsymbol{t}_{\alpha} \otimes \boldsymbol{E}_{\alpha} \pm \boldsymbol{e}_3 \otimes \boldsymbol{E}_3\}$, the mobile frame:

$$\boldsymbol{F}_{\boldsymbol{\Lambda}_{E_3}} : \boldsymbol{t}_3 \mapsto (\tilde{\boldsymbol{X}}_1 = (\sin\psi)^{-1}\partial_{\varphi}, \tilde{\boldsymbol{X}}_2 = \partial_{\psi}) \tag{5}$$

Finally, combining (2) and (4) shows that (φ, ψ, λ) realize the three Euler angles of a $3-1-3$ sequence. Hence, the two polar singularities of S^2 stand for those of any "three-angles" parameterization of $SO(3)$.

II.3 Kinematic model

II.3.1 Kinematics on $SO(3)$

The kinematics on $SO(3)$ is defined in the material and spatial settings (from left to right), by:

$$\boldsymbol{\Omega} = (\boldsymbol{R}^T.\dot{\boldsymbol{R}})^{\vee} = \Omega_i \boldsymbol{E}_i \quad , \quad \boldsymbol{\omega} = (\dot{\boldsymbol{R}}.\boldsymbol{R}^T)^{\vee} = \omega_i \boldsymbol{e}_i \tag{6}$$

Where $\boldsymbol{\Omega} \in so(3)$ (respectively: $\boldsymbol{\omega} \in so(3)$) is the material (respectively: spatial) angular velocity of the spacecraft.

With the proposed fibration of $SO(3)$, the kinematics split into those on the base manifold and in the fiber.

II.3.2 Kinematics on S^2

It is simply given by: $$\dot{\boldsymbol{t}}_3 = \boldsymbol{\omega} \times \boldsymbol{t}_3 = \Omega_2 \boldsymbol{t}_1 - \Omega_1 \boldsymbol{t}_2 = \left\langle \dot{\boldsymbol{t}}_3, \boldsymbol{t}_1 \right\rangle \boldsymbol{t}_1 + \left\langle \dot{\boldsymbol{t}}_3, \boldsymbol{t}_2 \right\rangle \boldsymbol{t}_2 \tag{7}$$

Then, any $\boldsymbol{\Lambda}_{\boldsymbol{E}_3}$ with any chart of S^2, parameterize (7).

II.3.3 Kinematics on the fiber

It is given by the following lemma:

Lemma 1 (proven in Appendix)

The kinematics around the non actuated axis is ruled by the following relation:

$$\Omega_3 = \dot{\lambda} + \boldsymbol{\omega}_{S^2}(\tilde{\dot{\boldsymbol{t}}}_3) \tag{8}$$

Where $\boldsymbol{\omega}_{S^2}$ is the rotation 1-form of the Levi-Civita connection of S^2 and $\tilde{\dot{\boldsymbol{t}}}_3 \in T_{\boldsymbol{t}_3} S^2$ is induced by $\dot{\boldsymbol{t}}_3 \in \mathbb{R}^3$.

II.4 Dynamic modeling

From Poincaré equations [15] applied to the satellite's configuration space: $SO(3) \times \mathbb{R}^2$, the spatial dynamics write as:

$$d(\boldsymbol{I}.\boldsymbol{\omega} + \tilde{\boldsymbol{I}}_r \dot{q})/dt = \boldsymbol{0} \qquad , \qquad d(\tilde{\boldsymbol{I}}_r^T.\boldsymbol{\omega} + \overline{J}_r \dot{q})/dt = \tau \tag{9}$$

With: $\tau = (\tau_1, \tau_2)^T$ the control torque vector, and the following inertia tensors: $\boldsymbol{I} = \boldsymbol{R}.\boldsymbol{J}.\boldsymbol{R}^T$, $\tilde{\boldsymbol{I}}_r = \boldsymbol{R}.\tilde{\boldsymbol{J}}_r$, $\boldsymbol{J} = \boldsymbol{J}_s + \boldsymbol{J}_r$, with: $\boldsymbol{J}_s = J_{si}\boldsymbol{E}_i \otimes \boldsymbol{E}_i$, $\boldsymbol{J}_r = J_{ri}\boldsymbol{E}_i \otimes \boldsymbol{E}_i$, $\tilde{\boldsymbol{J}}_r = J_{r\alpha}\boldsymbol{E}_{\alpha} \otimes dq^{\alpha}$, $\overline{J}_r = J_{r\alpha} dq^{\alpha} \otimes dq^{\alpha}$ ($i = 1,2,3$; $\alpha = 1,2$). Where the J_{si}'s are the principal inertia moments of the satellite (with its rotors), and the J_{ri}'s are those of the rotors around their own axis ($J_{r3} = 0$). Moreover, introducing the spatial and material (from left to right) angular moments:

$$\boldsymbol{\sigma} = \boldsymbol{I}.\boldsymbol{\omega} + \tilde{\boldsymbol{I}}_r\dot{q} \quad , \qquad \boldsymbol{p} = \boldsymbol{R}^T.\boldsymbol{\sigma} = \boldsymbol{J}.\boldsymbol{\Omega} + \tilde{\boldsymbol{J}}_r\dot{q} \, , \tag{10}$$

Allows rewriting (9.a) as the conservation law:

$$\boldsymbol{\sigma} = \boldsymbol{\sigma}(t_o) = \boldsymbol{\sigma}_o \tag{11}$$

While in the material setting, (9) rewrites as:

$$\dot{\boldsymbol{p}} + \boldsymbol{\Omega} \times \boldsymbol{p} = \boldsymbol{0} \quad , \quad \tilde{\boldsymbol{J}}_r^T.\dot{\boldsymbol{\Omega}} + \bar{J}_r\ddot{q} = \tau \tag{12}$$

III. OPEN LOOP CONTROL DESIGN

We first define the admissible state space of the spacecraft attitude, i.e. the sub-manifold of $\boldsymbol{x} = (\boldsymbol{R}, \boldsymbol{\Omega}) \in TSO(3)$ compatible with (10).

III.1 Admissible space

Because of the symmetry of the system with respect to the axe of poles, we place $(O, \boldsymbol{e}_1, \boldsymbol{e}_2, \boldsymbol{e}_3)$ such that:

$$\boldsymbol{\sigma}_o = \langle \boldsymbol{\sigma}_o, \boldsymbol{e}_3 \rangle \boldsymbol{e}_3 = \sigma_{o\,3}\boldsymbol{e}_3 \tag{13}$$

Lemma 2

The admissible space $\mathcal{A}$ of the spacecraft attitude is a five dimensional sub-manifold of the tangent bundle $TSO(3) \cong SO(3) \times so(3)$. Moreover, with (13), it is defined by (with: $A = \sigma_{o\,3} / J_3$):

$$\mathcal{A} = \{\boldsymbol{x} \in TSO(3) / \Omega_3 = A\langle \boldsymbol{t}_3, \boldsymbol{e}_3 \rangle\} \tag{14}$$

Proof

First, equalize (10.b) with $R^T.\boldsymbol{\sigma}_o$ and then project the result onto $\boldsymbol{E}_3$. Then (13) gives the following constraint on $TSO(3)$:

$$\Omega_3 = A\langle \boldsymbol{t}_3, \boldsymbol{e}_3 \rangle \tag{15}$$

which is non-holonomic since Ω_3 is a non-integrable 1-form.

III.2 Control objectives

We are now going to define two control objectives relevant with applications and compatible with (15).

Objective 1: O.1

We first focus our interest on target states for which the spacecraft is at rest. This objective is particularly relevant with respect to practical aiming applications. It is defined by the space of admissible attitudes at rest:

$$(\mathcal{A}_1 \subset \mathcal{A}) := \{\boldsymbol{x} \in TSO(3) / A\langle \boldsymbol{t}_3, \boldsymbol{e}_3 \rangle = 0, \boldsymbol{\Omega} = \boldsymbol{0}\} \tag{16}$$

Note that when $A = 0$ (i.e. $\boldsymbol{\sigma}_o = \boldsymbol{0}$), $SO(3)$ is wholy accessible at rest.

Objective 2: O.2

Alternatively, it can be interesting to steer the spacecraft to an arbitrary desired final orientation $\boldsymbol{R}_f \in SO(3)$. In this case, with $\Omega_{\alpha f} = 0$ ($\alpha = 1,2$), (15) forces the satellite to spin around its non-actuated axis with the velocity $\Omega_{3f} = A\langle \boldsymbol{t}_{3f}, \boldsymbol{e}_3 \rangle$. This second set of objectives realizes the space of admissible states with a specified final orientation $\boldsymbol{R}_f$:

$$(\mathcal{A}_2 \subset \mathcal{A}) := \{\boldsymbol{x} \in TSO(3) / \Omega_\alpha = 0, \Omega_3 = A\langle \boldsymbol{t}_3, \boldsymbol{e}_3 \rangle\} \tag{17}$$

Finally, in the following, we shall denote by $\mathcal{A}^\circ$ and $\mathcal{A}_2{}^\circ$ respectively, the $\mathcal{A}$, and $\mathcal{A}_2$ spaces once privated of $T\mathcal{U}_\pm := \bigcup_{\boldsymbol{R} \in \mathcal{U}_\pm} T_{\boldsymbol{R}} SO(3)$. Moreover, if $A = 0$, $\mathcal{A}_1 = \mathcal{A}_2$, while in any case: $\mathcal{A}_1, \mathcal{A}_2{}^\circ \subset \mathcal{A}^\circ$.

III.3 Open loop control strategy

With these two objectives (O.1,2) the open loop control problem consists of finding a torque law that steers $\boldsymbol{x}$ from any initial state: $\boldsymbol{x}_o \in \mathcal{A}$, to any final one: $\boldsymbol{x}_f \in \mathcal{A}_1$ or $\mathcal{A}_2$. Its solution is based on the following theorem.

Theorem 1

If we now the time evolution of the non-actuated axis $\boldsymbol{t}_3$ on $S^2 - \{\pm \boldsymbol{e}_3\} = \mathcal{U}$, we can completely recover the time evolution of the states and outputs (here the control torques).

Proof

From (4), a given time evolution: $\boldsymbol{t}_3(.)$ on $\mathcal{U}$, fixes: $\boldsymbol{\Lambda}_{\boldsymbol{E}_3}(\boldsymbol{t}_3(.))$. Moreover (15) gives $\Omega_3(.)$, and by (8), $\dot{\lambda}(.)$. Time integrating $\dot{\lambda}(.)$ gives $\lambda(.)$. Then, (2) gives the motion attitude $\boldsymbol{R}(.)$ on $\mathcal{V}$ from which, we find : $\boldsymbol{\Omega}(.)$ (from (7)), and : $\boldsymbol{p}(.) = \boldsymbol{R}^T(.).\boldsymbol{\sigma}_o$. Next, from (10.b) we deduce $\dot{q}(.)$ and by time integration $q(.)$. Then, (10.b) and (12.a) give $\dot{\boldsymbol{p}}(.)$, which once combined with the time differential of (7), gives the $\dot{\Omega}_\alpha(.)$'s. Introducing them into (12.b) finally gives:

$$\tau_1 = -J_{s1}\dot{\Omega}_1 - \langle \boldsymbol{E}_1, \boldsymbol{\Omega} \times \boldsymbol{p} \rangle \quad , \quad \tau_2 = -J_{s2}\dot{\Omega}_2 - \langle \boldsymbol{E}_2, \boldsymbol{\Omega} \times \boldsymbol{p} \rangle \tag{18}$$

where, $J_{s\alpha} = J_\alpha - J_{r\alpha}$. Finally, we recover the time evolution of all internal and external variables[2]. **q.d.m.**

III. 4 Path planning strategy

Let us consider any $\boldsymbol{x}_o$, $\boldsymbol{x}_f \in \mathcal{A}^\circ$, and their corresponding: $((\boldsymbol{t}_{3o}, \dot{\boldsymbol{t}}_{3o}), (\lambda_o, \dot{\lambda}_o))$ and $((\boldsymbol{t}_{3f}, \dot{\boldsymbol{t}}_{3f}), (\lambda_f, \dot{\lambda}_f))$ on $T\mathcal{U} \times TSO(2)$. Then, any desired motion $\boldsymbol{t}_{3d}(.) : [t_o, t_f] \subset \mathbb{R}^+ \mapsto \boldsymbol{t}_{3d}(t) \in \mathcal{U}$: of $\boldsymbol{t}_3$, s.t.: $\boldsymbol{t}_{3d,o} = \boldsymbol{t}_{3o}$, $\dot{\boldsymbol{t}}_{3d,o} = \dot{\boldsymbol{t}}_{3o}$, $\boldsymbol{t}_{3d,f} = \boldsymbol{t}_{3f}$, $\dot{\boldsymbol{t}}_{3d,f} = \boldsymbol{0}$; solves the path planning if it also verifies:

$$\lambda_f - \lambda_o = \Delta\lambda_f = \int_{t_o}^{t_f} A\langle \boldsymbol{t}_{3d}, \boldsymbol{e}_3 \rangle dt - \int_{\boldsymbol{t}_{3d}(.) \subset \mathcal{U}} \boldsymbol{\omega}_{S^2}(\tilde{\dot{\boldsymbol{t}}}_{3d}), \tag{19}$$

[2] It is worth noting that because this reconstruction process requires some time integration, the position of the non-actuated axis on the unit sphere does not realize a set of flat outputs.

Moreover, from *theorem 1*, the accessibility of $\mathcal{A}_1$ and $\mathcal{A}_2^\circ$ from $\mathcal{A}^\circ$ is proved. Finally, the accessibility is conditioned by the verification of (19) where the presence of $\boldsymbol{\omega}_{S^2}$ shows that it is the curvature of S^2 which generates the non-actuated rotation. Moreover, when $\boldsymbol{\sigma}_o = \mathbf{0}$, the existence of admissible paths on $\mathcal{U}$ producing any desired shift $\Delta\lambda_f$ in the fiber, is guaranteed by: $\mathcal{H}ol(S^2) = SO(2)$. Where $\mathcal{H}ol(S^2)$ is the holonomy group of S^2 [14], and $\Delta\lambda_f$ stands for a "geometric phase". In the general case: $\boldsymbol{\sigma}_o \neq 0$, the first integrand of (19) ads a "dynamic phase" to the geometric one [2].

IV. RESTRICTED ACCESSIBILITY

We first investigate the (restricted) accessibility of $\mathcal{A}_1$, $\mathcal{A}_2^\circ$ from $\mathcal{A}^\circ$. It is based on the stereo-graphic projection [16].

IV.1 The stereo-graphic projection (figure 2)

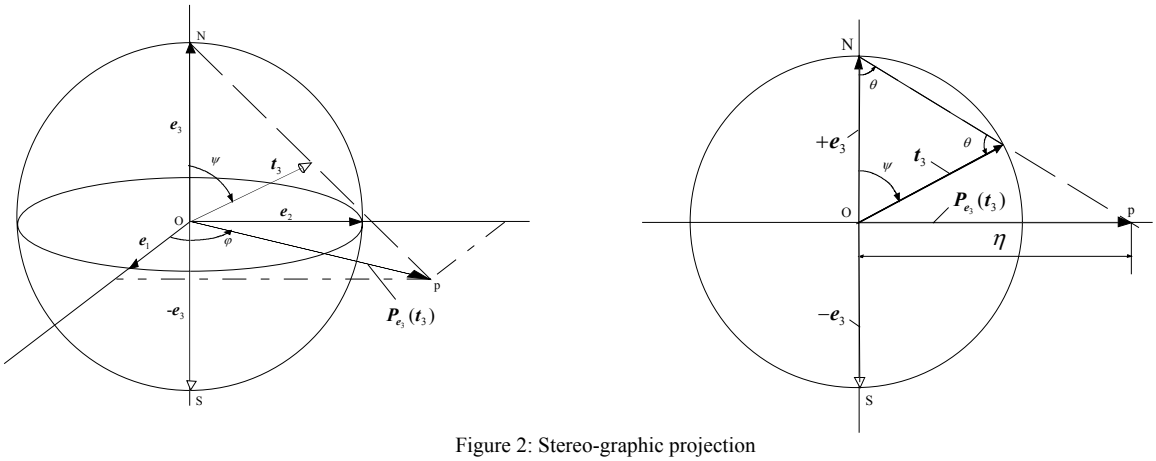

Figure 2: Stereo-graphic projection

From planar geometric considerations (see figure 2), we have, with $\boldsymbol{P}_{e_3}(\boldsymbol{t}_3)$ the projection of $\boldsymbol{t}_3$ from $\boldsymbol{e}_3$ in the equatorial plane and: $\eta = \left\langle \boldsymbol{P}_{e_3}(\boldsymbol{t}_3), \boldsymbol{P}_{e_3}(\boldsymbol{t}_3) \right\rangle^{1/2} = \left\| \boldsymbol{P}_{e_3}(\boldsymbol{t}_3) \right\|$:

$$\cos\psi = (\eta^2 - 1)(\eta^2 + 1)^{-1}, \qquad \sin\psi = 2\eta(\eta^2 + 1)^{-1} \tag{20}$$

Thus, $(\mathcal{U}, \eta, \varphi)$ realizes a chart of S^2.

IV.2 Path planning

Because (19) is invariant by any rotation around the symmetry axis of poles, we take as reference variables (from which we can recover all the internal and external variables):

$$\eta, \quad \text{and:} \quad \xi = \dot{\varphi}/(1+\eta^2) \tag{21}$$

Hence, with $t_f = +\infty$, the desired time evolutions $\eta_d(.)$ and $\xi_d(.)$ have to verify the two integral conditions:

$$\varphi_f - \varphi_o = \Delta\varphi_f = \int_{t_o}^{+\infty} (1+\eta_d^2)\xi_d dt \ , \qquad \lambda_f - \lambda_o = \Delta\lambda_f = \int_{t_o}^{+\infty} (A(1+\eta_d^2)^{-1} - \xi_d)(\eta_d^2 - 1)dt = J_f - \int_{t_o}^{+\infty} \xi_d(\eta_d^2 - 1)dt \tag{22}$$

Where the second, is a parameterization of (19) by (21) with J_f denoting the "dynamic phase".

Plus, the boundary conditions:

$$\eta_{d,o} = \eta_o, \ \dot{\eta}_{d,o} = \dot{\eta}_o, \ \eta_{d,f} = \eta_f, \ \dot{\eta}_{d,f} = \ddot{\eta}_{d,f} = 0 \tag{23}$$

$$\xi_{d,o} = \xi_o = \dot{\varphi}_o / \eta_o \,, \quad \xi_{d,f} = \dot{\xi}_{d,f} = \xi_f = \dot{\xi}_f = 0 \tag{24}$$

with $\eta_o > 0$ and η_f bounded , since: $\boldsymbol{t}_{3o}$, $\boldsymbol{t}_{3f} \in \mathcal{U}$. Then, we have the following theorem.

IV.3 Theorem 2: Accessibility of $\mathcal{A}_1$ and $\mathcal{A}_2^\circ$ from $\mathcal{A}^\circ$

With the following time evolution for (21):

$$\eta_d(t) = a_o + \sum_{i=1}^{2} a_i e^{-\lambda_i t} \,, \qquad \xi_d(t) = b_o + \sum_{j=1}^{3} b_j e^{-\beta_j t} \tag{25}$$

There always exist two sets of bounded real parameters $(a_i, \lambda_i)_{i=o,1,2}$ and $(b_j, \beta_j)_{j=o,1,2,3}$, (with the λ_i 's and β_j 's positive and distinct) such that (22-24) are verified under the constraint: $\eta > 0$. Moreover, $\mathcal{A}_1$ and $\mathcal{A}_2^\circ$ are accessible from $\mathcal{A}^\circ$.

Proof

It requires invoking the following lemma.

Lemma 3

For any initial conditions η_o and $\dot{\eta}_o$ and any desired final value $\eta_f > 0$, there exist sufficiently high λ_1 and λ_2 such that the trajectory $\eta_d(.)$ defined by (25.a) and (23) is such that $\eta_d(t) > 0$ for all $t \neq 0$.

Equations (23) impose to the a_i 's to satisfy (with $a_o = \eta_f$):

$$\begin{pmatrix} e^{-\lambda_1 t_o} & e^{-\lambda_2 t_o} \\ -\lambda_1 e^{-\lambda_1 t_o} & -\lambda_2 e^{-\lambda_2 t_o} \end{pmatrix} \begin{pmatrix} a_1 \\ a_2 \end{pmatrix} = \begin{pmatrix} \eta_o - \eta_f \\ \dot{\eta}_o \end{pmatrix} , \tag{26}$$

where, λ_1 and λ_2 being distinct, (26) is always invertible. Moreover, from the *lemma 3* there always exist λ_1 and λ_2 s.t.: $\eta(t) > 0$, $\forall t \in [t_o, +\infty[$. Once $\eta_d(.)$ known, we calculate the dynamic phase J_f of (22.b). Finally, (23) and (24) impose to the b_i 's, to satisfy (with $b_o = 0$):

$$\begin{pmatrix} e^{-\beta_1 t_o} & e^{-\beta_2 t_o} & e^{-\beta_3 t_o} \\ e^{-\beta_1 t_o}/\beta_1 & e^{-\beta_2 t_o}/\beta_2 & e^{-\beta_3 t_o}/\beta_3 \\ B_{31} & B_{32} & B_{33} \end{pmatrix} \begin{pmatrix} b_1 \\ b_2 \\ b_3 \end{pmatrix} = \begin{pmatrix} \xi_o \\ (1/2)(\Delta\lambda_f + \Delta\varphi_f - J_f) \\ \Delta\varphi_f - ((1+\eta_f^2)/2)(\Delta\lambda_f + \Delta\varphi_f - J_f) \end{pmatrix} \tag{27}$$

with: $B_{3j} = 2\eta_f \sum_{i=1}^{2} a_i \frac{e^{-(\lambda_i+\beta_j)t_o}}{(\lambda_i+\beta_j)} + \sum_{i,k=1}^{2} a_i a_k \frac{e^{-(\lambda_i+\lambda_k+\beta_j)t_o}}{(\lambda_i+\lambda_k+\beta_j)}$. Since the λ_i 's and the β_i 's are distinct and arbitrary, (27) is singular only when $a_1 = a_2 = 0$. This corresponds to a path singularity that will be dealt with, in subsection V.1. Finally, from $\xi_d(.)$

and $\eta_d(.)$, we find $\varphi_d(.)$ and $\lambda_d(.)$, and from (3), (21), and (20) we find $\boldsymbol{t}_{3d}(.)$. Then, from *theorem 1*, we recover the desired control torques (18) which steer the satellite from any state of $\mathcal{A}^\circ$ to any one of $\mathcal{A}_1$ or $\mathcal{A}_2^\circ$. **q.d.m.**

V. GLOBAL ACCESSIBILITY

In order to extend the accessibility to the whole unit sphere of $\mathcal{A}_2$ and $\mathcal{A}$, we have to deal with the singularities of the parameterization (η, ξ) of the paths on the unit sphere.

V.1 Path singularities

As mentioned earlier, with $\eta_o = \eta_f$, and $\dot{\eta}_o = 0$, (26) imposes: $a_1 = a_2 = 0$, so making (27) singular. In order to circumvent this path singularity, take a piece-wise continuous time evolution $\eta_d(.)$ defined as follows:

1°) $t < t_i$: $\eta_d(.)$ is given by (25.a)-(26) with: $\eta_f = \eta_i$.

2°) $t \geq t_i$: $\eta_d(.)$ given by (25.a)-(26) with: $(\eta_o, \dot{\eta}_o) = (\eta_i, 0)$.

Where "$\eta = \eta_i (\neq \eta_o = \eta_f)$" is an intermediate circle on which $\boldsymbol{t}_3$ transits, and for any $\varepsilon > 0$, $t_i = t_i(\varepsilon)$ is s.t.: $\sup\left(\left|\eta_d(t) - \eta_i\right|, \left|\dot{\eta}_d(t)\right|\right) \leq \varepsilon$, $\forall t \geq t_i$. Finally, $\xi_d(.)$ is still given by (25.b), with the b_i's fixed by (24), (27), with (22) now piece-wising computed.

V.2 Polar singularities

V.2.1 Continuation of the path planing to the south pole

On the north pole ($+\boldsymbol{e}_3$): $\eta = +\infty$, so making unfeasible any path (25) starting or arriving at $+\boldsymbol{e}_3$. However, on $-\boldsymbol{e}_3$:

$$\eta = 0\,, \quad \dot{\eta} = (1/2)\left\| \dot{\boldsymbol{t}}_3 \right\| = (1/2)\sqrt{\Omega_1^2 + \Omega_2^2}\,, \qquad \varphi - \lambda = \arctan\left(\left\langle \boldsymbol{t}_1, \boldsymbol{e}_2 \right\rangle, \left\langle \boldsymbol{t}_1, \boldsymbol{e}_1 \right\rangle\right), \qquad \dot{\lambda} - \xi = \Omega_3\,, \tag{28}$$

And so (25.a) can be continuously prolonged to $-\boldsymbol{e}_3$ as starting point, with initial conditions:

$$\eta_o = 0\,, \quad \dot{\eta}_o = (1/2)\sqrt{\Omega_{1o}^2 + \Omega_{2o}^2}\,, \quad \xi_o = 0\,, \quad \varphi_o = 0 \tag{29}$$

Moreover, fixing the final conditions:

$$\eta_f = 0\,, \quad \xi_f = 0\,, \quad \varphi_f = 0\,, \tag{30}$$

continuates (25.a) to $-\boldsymbol{e}_3$ as arriving point. Furthermore, (29)-(30) fixe $\Delta\varphi_f$ and $\Delta\lambda_f$ in (27). Finally, from the *lemma 3*, such a continuation is always possible with: $\eta(t) \geq 0$, $\forall t \in [t_o, +\infty[$.

V.2.2 Antipodal stereo-graphic projection

To circumvent the north pole singularity ($+\boldsymbol{e}_3$), let us introduce $\boldsymbol{P}_{-\boldsymbol{e}_3}(.)$, the stereo-graphic projection from the south pole ($-\boldsymbol{e}_3$). It defines a new coordinate η_- (instead of $\eta = \eta_+$) related to the angle: $\psi_- = \pi - \psi_+$ (where: $\psi = \psi_+$), as η_+ is related

to ψ_+. Hence, inserting $\psi_+ = \pi - \psi_-$ into (3) and (4), with ψ_- defined by: $\cos\psi_- = (\eta_-^2 - 1)(\eta_-^2 + 1)^{-1}$, and $\sin\psi_- = 2\eta_-(\eta_-^2 + 1)^{-1}$, gives a new parameterization of $\boldsymbol{R}$ which is now defined at $+\boldsymbol{e}_3$ and singular at $-\boldsymbol{e}_3$.

V.3 Global path planning - accessibility of $\mathcal{A}_1$ and $\mathcal{A}_2$ from $\mathcal{A}$

We are now going to prove the following theorem. It is based on the previous continuation, and the two stereo-graphic projections with their set of reference variables: $(\eta_+, \xi_+ = \dot{\varphi}/\eta_+)$ and $(\eta_-, \xi_- = \dot{\varphi}/\eta_-)$.

Theorem 3

There always exist some time evolutions (25) or one of its piece-wise combination (V.1) applied to (η_+, ξ_+) or (and) (η_-, ξ_-) steering the satellite from any $\boldsymbol{x}_o$ of $\mathcal{A}$ to any $\boldsymbol{x}_f$ of $\mathcal{A}_1$ or $\mathcal{A}_2$.

Proof

Let us first introduce the four following state spaces: $\mathcal{A}_\pm := T\mathcal{U}_\pm \cap \mathcal{A}$ and $\mathcal{A}_{2\pm} := T\mathcal{U}_\pm \cap \mathcal{A}_2$. Where $\mathcal{A}_\pm$ (respect., $\mathcal{A}_{2\pm}$) are the two sub-spaces of $\mathcal{A}$ (respect, of $\mathcal{A}_2$), s.t. $\boldsymbol{t}_3 = \pm\boldsymbol{e}_3$. Therefore, because of *theorem 2*, and: $\mathcal{A} = \mathcal{A}^\circ \cup \mathcal{A}_+ \cup \mathcal{A}_-$, $\mathcal{A}_2 = \mathcal{A}_2{}^\circ \cup \mathcal{A}_{2+} \cup \mathcal{A}_{2-}$, the *theorem* 3 is proved by the fact that:

1°) $\mathcal{A}_1$ and $\mathcal{A}_2{}^\circ$ are accessible from $\mathcal{A}_-$ (respect. $\mathcal{A}_+$), by applying the path (25) with initial conditions (29) to (η_+, ξ_+) (respect., to (η_-, ξ_-)).

2°) $\mathcal{A}_{2-}$ (respect., $\mathcal{A}_{2+}$) is accessible from $\mathcal{A}^\circ$, by applying (25) with (30) to (η_+, ξ_+) (respect., to (η_-, ξ_-)).

3°) $\mathcal{A}_{2+}$ and $\mathcal{A}_{2-}$ are accessible from $\mathcal{A}_+$ and $\mathcal{A}_-$, i.e. (22.b) can be satisfied while steering $\boldsymbol{t}_3$: *a*) from one pole to itself; *b*) from one pole to the other. As a matter of fact:

3.a) In the first sub-case (*a*), if the pole is the south pole (respect. the north one) apply (25), with initial and final conditions (29) and (30) to (η_+, ξ_+) (respect. to (η_-, ξ_-)). From (29) and (30), a path singularity occurs. In order to escape from it, use the piece-wise combination of V.1.

3.b) In the second sub-case (*b*), if starting from the south pole (respect. the north one) apply (25) with (29) to (η_+, ξ_+) (respect. to (η_-, ξ_-)) and then transit on the equator by imposing $\eta_{+i} = 1$ (respect. $\eta_{-i} = 1$) (see V.1). While transiting on the equator, take benefit of the symmetry property: $\eta_{+i} = \eta_{-i} = 1$; in order to change η_+ into η_- (respect. η_- into η_+), and steer the satellite to the north pole (respect. the south) with η_- (respect. η_+) fixed by (30), and initial regular conditions fixed by the transition. **q.d.m.**

VI. SIMULATION RESULTS

All the numerical examples are based on the following datas:

$$(J_{s1}, J_{s2}, J_{s3}) = (300, 200, 290)\ kg.m^2\ ,\ J_{r1} = J_{r2} = 10 kg.m^2$$

We now report two simulation results of the control law (18) with the previous path planning. The first test deals with the control objective O.1, the second with O.2. The first test concerns a regular case while the second exhibits the most perverse case when going from one pole to the other.

Test 1: O.1, regular case

The conditions of the test are the following:

$t_f = 1500$, $\beta_1 = 10\beta_2 = 100\beta_3 = 5\lambda_1 = 50\lambda_2 = 0.5$, $\psi_o = 3\pi/4$, $\psi_f = 2\varphi_o = 2\lambda_o = \pi/2$, $\varphi_f = \lambda_f = 0$, $\dot{q}_{1o} = -\dot{q}_{2o} = 10$, and $\boldsymbol{\sigma}_o = 0.6\,\boldsymbol{e}_3$.

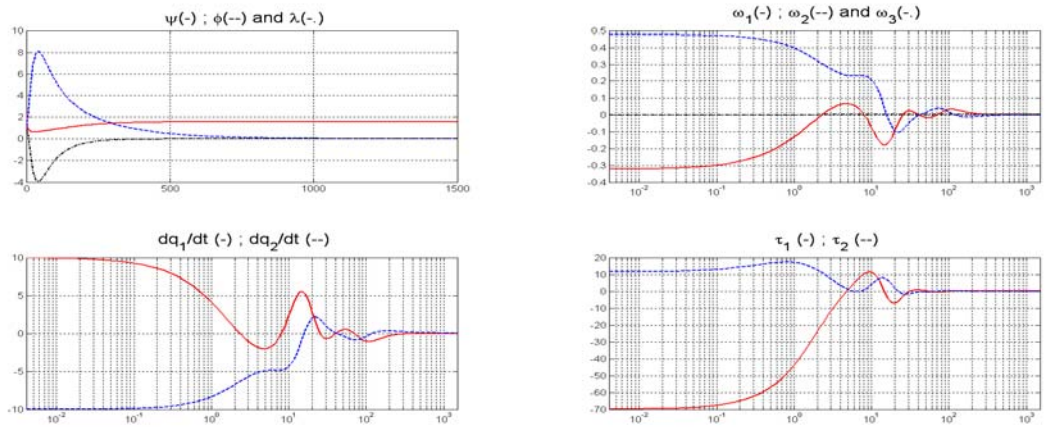

Figure 3: O.1 in the regular case

Test 2: O.2, singular case

The conditions of the test are the following: $t_f = 1.10^4$, $t_i = t_f/2$, $\beta_1 = 10\beta_2 = 100\beta_3 = \lambda_1 = 10\lambda_2 = 0.1$, $\psi_o = \pi$, $\lambda_o = 3\pi/2$, $\varphi_o = \psi_f = \varphi_f = \lambda_f = 0$, $\dot{q}_{o1} = -\dot{q}_{o2} = 10$, $\boldsymbol{\sigma}_o = 0.6\,\boldsymbol{e}_3$.

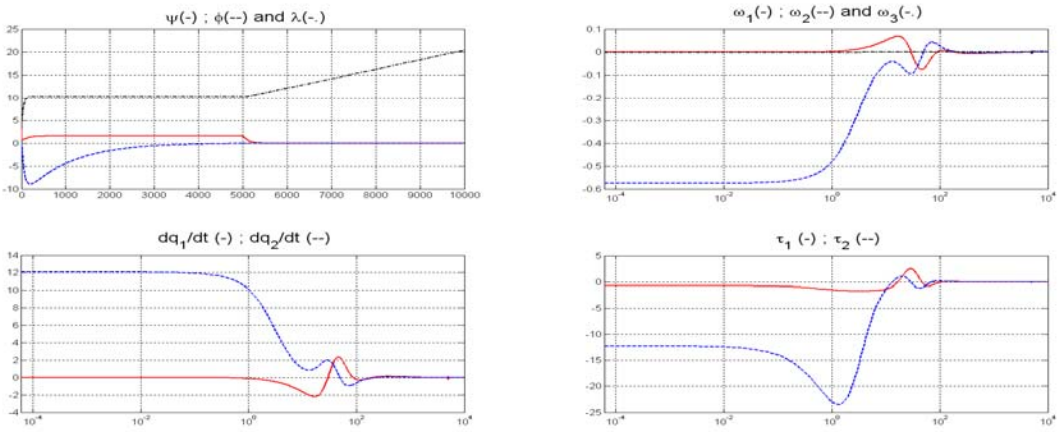

Figure 4: O.2 in the singular case

VII. CONCLUSION

The article proposes some constructive and explicit solutions to the open loop control problem of steering the attitude of a two-wheeled satellite from any admissible state to two sets of objectives compatible with the momentum conservation and one rotor failure. For these two objectives, the path planning is based on the same strategy. First, the time evolution of two reference variables describing the motion of the non-actuated axis on the unit sphere are fixed in order to verify some boundary conditions and the conservation of the angular momentum; second, all the internal and control variables are recovered from these two variables. Geometrically, it is the curvature of the unit sphere that allows recovering the lost actuated degree of freedom. The reference variables are deduced of two antipodal stereo-graphic projections and reduced on a truncated basis of exponentials whose the basis parameters are computed explicitly. Finally, many works have to complete this first one. First, the open loop control here proposed will be used in a second time to achieve a non-smooth feedback law based on a receding horizon strategy [17]. Second, on the base of this feedback control law, the problem of the robustness will be treated. About that point, let us remark that the satellite with two wheels does not pose the robustness problem in a standard manner. As a matter of fact, the incertitude on inertia parameters or the presence of external perturbing torques modifies the angular momentum conservation law, and consequently, the accessible control objectives.

REFERENCES

1. Tsiotras, P., Doumtchenko, V., "Control of spacecraft subject to actuator failures: State-of-the-Art and Open Problems", Journal of Astronautical Sciences, Vol. 48, Nos. 2 and 3, pp. 337-358, 2000.
2. Montgomery, R., "Gauge theory and the falling cat", in Michael J. Enos, editor, Dynamics and control of mechanical systems: the falling cat and related problems. American Mathematical Society, Providence, R.I., 1992.
3. Bonnard, B., "Controllabilité des systèmes mécaniques sur les groupes de Lie", SIAM Journal on Control and Optimization, 22(5), 1984, pp. 711-722.
4. Crouch, P.E., "Spacecraft attitude control and stabilization: Applications of geometric control theory to rigid body models", IEEE Transactions on Automatic Control, Vol. 29, No. 4, 1984, pp. 321-331.
5. Morin, P., Samson, C., Pomet, J.B. and Jiang, Z.P., "Time varying feedback stabilization of a rigid spacecraft with two controls", Systems and Control Letters, 25, 1995, pp. 375-385.
6. Coron, J.M., Kerai, E.Y., "Explicit feedbacks stabilizing the attitude of a rigid spacecraft with two control torques", Automatica, 32(5), 1996, pp. 669-677.
7. Alamir, M., Boyer, F., "Fast generation of attractive trajectories for an under-actuated satellite, application to feedback control design" Optimization and Engineering, 4, 2003, pp. 215-230.
8. Krishnan, H., Mc Clamroch, N.H., Reyhanoglu, M., "Attitude stabilization of a rigid spacecraft using two momentum wheel actuators", Journal of Guidance, Control and Dynamics, 18(2), 1995, pp. 256-263.
9. Horri, N.M., Hodgart, S., "Attitude stabilization of an underactuated satellite using two wheels" IEEEAC conf. , 2002, Vol. 6, pp. 2629-2635.
10. Fliess, M., Lévine, J., Martin, Ph., Rouchon, P., "Flatness and defect of nonlinear systems: introductory theory and examples", Int. Journal of Control, 44(5), 1999, pp. 922-937.
11. Walsh, G.C., Montgomery, R., Sastry, S.S., « Orientation control of an underactuated rigid satellite » , Proceedings of the American Control Conference, pp. 1312-1316, 1993.
12. Tsiotras, P., Luo, J., "Control of Underactuated Spacecraft with Bounded Inputs", Automatica, Vol. 36, No. 8, 2000, pp. 1153-1169.
13. Alekseevskij, D.V., Vinogradov, A.M., Lychagin, V.V., "Basic Ideas and concepts of differential geometry", Encyclopedia of Mathematical Sciences, Vol. 28, R.V. Gamkrelidze (Ed.), Tome 1 : Geometry, Springer-Verlag, 1991.
14. Cartan E., "Leçons sur la géométrie des espaces de Riemann", Editions Gauthier-Villars, Paris, 1946 (in French).
15. Poincaré, H., 'Sur une forme nouvelle des équations de la mécanique', Comptes rendus de l'Académie des Sciences de Paris, (132), pp. 369-371, 1901, (in French).
16. Berger, M., « Géometrie », Tome 2, ed. Nathan, Paris, 1992, (in French).
17. Alamir, A., Marchand, N., « Numerical stabilisation of non-linear systems : Exact theory and approximate numerical implementation », European Journal of Control, 5, 1999, pp. 87-97.

APPENDIX

Proof of lemma 1

Let us write the second term of (8), in the mobile frame $\boldsymbol{F}_{\boldsymbol{\Lambda}_{E_3}}$ defined by (5):

$$\boldsymbol{\omega}_{S^2}(\tilde{\dot{\boldsymbol{t}}}_3) = \boldsymbol{\omega}_{S^2}(\tilde{V}_\alpha \tilde{\boldsymbol{X}}_\alpha) = \tilde{V}_\alpha \boldsymbol{\omega}_{S^2}(\tilde{\boldsymbol{X}}_\alpha)$$

Where $(\tilde{V}_\alpha)_{\alpha=1,2}$ are the components of $\tilde{\dot{\boldsymbol{t}}}_3$ in $\boldsymbol{F}_{\boldsymbol{\Lambda}_{E_3}}$. Because $\boldsymbol{F}_{\boldsymbol{\Lambda}_{E_3}}$ is orthonormed, we have [14]:

$$\boldsymbol{\omega}_{S^2}(\tilde{\boldsymbol{X}}_1) = \left\langle [\tilde{\boldsymbol{X}}_1, \tilde{\boldsymbol{X}}_2], \tilde{\boldsymbol{X}}_1 \right\rangle_{S^2}, \boldsymbol{\omega}_{S^2}(\tilde{\boldsymbol{X}}_2) = \left\langle [\tilde{\boldsymbol{X}}_1, \tilde{\boldsymbol{X}}_2], \tilde{\boldsymbol{X}}_2 \right\rangle_{S^2}$$

Where [,] is the Lie Bracket and "$\langle\ ,\ \rangle_{S^2}$" is the metric induced by $\langle\ ,\ \rangle$ on S^2. Then, we have:

$$[\tilde{\boldsymbol{X}}_1, \tilde{\boldsymbol{X}}_2] = [(\sin\psi)^{-1}\partial_\varphi, \partial_\psi] = \cos\psi(\sin\psi)^{-2}\partial_\psi = \cot\psi\tilde{\boldsymbol{X}}_1$$

And so: $$\boldsymbol{\omega}_{S^2}(\tilde{\boldsymbol{X}}_1) = \left\langle \cot\psi\tilde{\boldsymbol{X}}_1, \tilde{\boldsymbol{X}}_1 \right\rangle_{S^2} = \cot\psi \ , \ \boldsymbol{\omega}_{S^2}(\tilde{\boldsymbol{X}}_2) = 0$$

But because : $$\boldsymbol{\omega}_{S^2}(\tilde{\boldsymbol{X}}_1) = \boldsymbol{\omega}_{S^2}((\sin\psi)^{-1}\partial_\varphi) = (\sin\psi)^{-1}\boldsymbol{\omega}_{S^2}(\partial_\varphi) \ , \ \boldsymbol{\omega}_{S^2}(\tilde{\boldsymbol{X}}_2) = \boldsymbol{\omega}_{S^2}(\partial_\psi)$$

We then have: $$\boldsymbol{\omega}_{S^2}(\partial_\varphi) = \sin\psi \ \boldsymbol{\omega}_{S^2}(\tilde{\boldsymbol{X}}_1) = \cos\psi \ , \quad \boldsymbol{\omega}_{S^2}(\partial_\psi) = 0$$

Hence, the connection 1-form is written in the spherical chart as: $\boldsymbol{\omega}_{S^2} = \cos\psi \, d\varphi$. Hence, we obtain in the same chart:

$$\boldsymbol{\omega}_{S^2}(\tilde{\dot{\boldsymbol{t}}}_3) = \boldsymbol{\omega}_{S^2}(\dot{\varphi}\,\partial_\varphi + \dot{\psi}\,\partial_\psi) = \cos\psi\dot{\varphi} \tag{A.1}$$

On the other side, let us parameterize (6) by the 1-3-1 sequence of Euler angles (φ, ψ, λ), simple computations give:

$$\Omega_3 = \left\langle \boldsymbol{\Omega}, \boldsymbol{E}_3 \right\rangle = \dot{\lambda} + \cos\psi\dot{\varphi}$$

Where we recognize (A.1). **q.d.m.**

Proof of lemma 3

Simple computation leads to the following expression of $e(t) = \eta(t) - \eta_f$ in the case where $\lambda_1 = (1/2)\lambda_2 = \lambda$:

$$e(t) = a(t)e(0) + (1/\lambda)(a(t) - e^{-\lambda t})\dot{\eta}_o \tag{A.2}$$

where $a(t) = 2e^{-\lambda t} - e^{-2\lambda t}$ which is a strictly decreasing positive function that is < 1 for all $t > 0$. Therefore, all we have to prove is that $e(t) > -\eta_f$ for all $t > 0$. Two situations are to be distinguished: 1) if $\dot{\eta}_o \geq 0$ then $e(t) \geq a(t)e(0)$ which meets the required condition given the property of $a(t)$. 2) If $\dot{\eta}_o < 0$, then one necessarily has $\eta(0) > 0$ (one cannot go beyond the north pole) and hence $e(0) = \delta - \eta_f$ for some $\delta > 0$. Taking $\lambda > 0$ sufficiently high in order to have $(1/\lambda)|\dot{\eta}_o| < \delta/2$, equation (A.2) writes:

$$e(t) \geq a(t)(\delta/2 - \eta_f) + (\delta/2)e^{-\lambda t} \tag{A.3}$$

which is greater than $-\eta_f$ for all *t*. This ends the proof. **q.d.m.**